Currents in Pharmaceutical Research (CPR)
Volume 1 Issue 1, Spring 2023
ISSN$_{(P)}$: 3007-3235 ISSN$_{(E)}$: 3007-3243
Homepage: https://journals.umt.edu.pk/index.php/cpr

Article QR

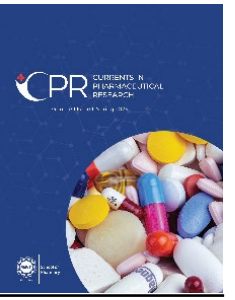

Title:	**Evaluation of Near-Infrared Chemical Imaging (NIR-CI) for the Authentication of Antibiotics**
Author (s):	Sulaf Assi[1], Sarah Rowlands[1], Panos Liatsis[2], Mana Al Hamid[3], Jamila Mustafina[4], Maitham Ghaly Yousif[5], Thomas Coombs[6], Dhiya Al-Jumeily OBE[7]
Affiliation (s):	[1]Pharmacy and Biomolecular Sciences, Liverpool John Moores University, UK. [2]Khalifa University, Abu Dhabi, UAE [3]Forensic Medical Service Center in Najran, Najran, Saudi Arabia. [4]Kazan Federal University, Russia. [5]Al-Qadisiyah University, Al-Qadisiyah, Iraq. [6]University Hospital Dorset, Bournemouth, UK. [7]Computer Science and Mathematics, Liverpool John Moore University, UK.
DOI:	https://doi.org/10.32350/cpr.11.04
History:	Received: April 18, 2023, Revised: May 10, 2023, Accepted: May 18, 2023, Published: June 28, 2023
Citation:	Assi S, Rowlands S, Liatsis P, et al. Evaluation of Near-Infrared Chemical Imaging (NIR-CI) for the authentication of antibiotics. *Curr Pharma Res*. 2023;1(1):47–69. https://doi.org/10.32350/cpr.11.04
Copyright:	
Licensing:	
Conflict of Interest:	Author(s) declared no conflict of interest

A publication of
The School of Pharmacy
University of Management and Technology, Lahore, Pakistan

Evaluation of Near-Infrared Chemical Imaging (NIR-CI) for the Authentication of Antibiotics

Sulaf Assi[1], Sarah Rowlands[1], Panos Liatsis[2], Mana Al Hamid[3], Jamila Mustafina[4], Maitham Ghaly Yousif[5], Thomas Coombs[6], and Dhiya Al-Jumeily OBE[7*]

[1]Pharmacy and Biomolecular Sciences, Liverpool John Moores University, United Kingdom
[2]Department of Electrical Engineering and Technology, Khalifa University, Abu Dhabi, United Arab Emirates
[3]Forensic Medical Service Center in Najran, Saudi Arabia
[4]Kazan Federal University, Russia
[5]College of Science, Al-Qadisiyah University, Iraq
[6]University Hospital Dorset, Bournemouth, United Kingdom
[7]Computer Science and Mathematics, Liverpool John Moore University, United Kingdom

ABSTRACT

Counterfeit medicines represent a public health threat that results in treatment failure and may even have lethal effects in the worst-case scenario. Near-infrared Chemical Imaging (NIR-CI) offers an informative and in-depth tool for several applications in the pharmaceutical industry, particularly for medicine authentication. The current study aimed to authenticate antibiotic tablets using NIR-CI. These tablets were measured non-destructively using a near-infrared microscope within their blister packaging, without their blisters, sectioned and crushed. The results showed that there was no marked difference in measuring the tablets within or without their blister packaging. The mean spectra of tablets showed high correlation coefficient values against the active pharmaceutical ingredient, in case of authentic tablets. On the other hand, counterfeit tablets showed key differences from their authentic alternatives with low correlation coefficient values. More specifically, counterfeit tablets showed poor distribution of the active pharmaceutical ingredient and excipients. It has been proved from the results that NIR-CI process is an authentic process for the evaluation of counterfeit tablets, non-destructively.

Keywords: active pharmaceutical ingredient, blister packaging, chemical imaging, correlation, counterfeit medicines, excipients, near-infrared, spectroscopy, tablets

* Corresponding Author: d.aljumeily@ljmu.ac.uk

1. INTRODUCTION

Counterfeit medicines represent a public threat worldwide that can impact both the health and the economy [1]. The health threats associated with counterfeit medicines range from treatment ineffectiveness to lethal effects [2]. According to the World Health Organisation (WHO), "Spurious/ falsely-labelled/ falsified/ counterfeit (SFFC) medicines are medicines that are deliberately and fraudulently mislabelled with respect to identity and/ or source". In this respect, medicine counterfeiting can be involved in any class of medicines (essential versus non-essential), any types of medicines (branded/generic), and may also include products with no active pharmaceutical ingredients (APIs), wrong dose (overdose/under-dose) of APIs, wrong ingredients, and fake packaging [3].

It is worth differentiating counterfeit from substandard medicines. Substandard medicines are poor quality medicines that fail to fulfil the manufacturer's specification due to accidental defects in their manufacturing or storage [4, 5]. The medicine is substandard if it incurs an accidental defect in the manufacturing process. However, if the defect is deliberate; then, it is categorised as a counterfeit rather than a substandard medicine.

Consequently, both counterfeit and substandard medicines impact patient safety and public health. This urges the need to identify these medicines for any defects including defects in their chemical constituents (APIs and excipients) and physical properties. It is crucial in the cases of authentication, not only to understand the presence and concentration of chemical constituents but also to map the distribution of these constituents within a tablet, in order to ensure content uniformity. Poor content uniformity of tablets influences their treatment effectiveness adversely, especially if the patient takes a quarter or half a tablet to adjust the dose of therapy. In such cases, inconsistent distribution of chemical constituents affects the dose taken by the patients which, in turn, leads to under-dose or over-dose. Under- or over-doses of antibiotics may lead to antibiotic resistance or therapy failure. Therefore, it is important to characterise accurately the presence and distribution of constituents in each tablet as a key part of the authentication process.

According to WHO reports [6], a total of eight alerts related to falsified and sub-standard medicines occurred between January 2022 and January 2023, spanning over fifteen countries worldwide, as shown in Table 1.

SFFC medicines have a range of known and unknown side effects. Known side effects of SFFC medicines include causing harm to the individual patient (for example, delaying treatment for a condition), toxicity (poisoning the body), and other potential lethal effects. It is worth noting that these toxic/lethal effects are not limited to one country or one class of drugs but could be encountered anywhere and with any drug class (Table 1). Hence, medicines reported to WHO include anaesthetics, anticancer, anti-infective, cough sedatives, hormone replacement therapy, and neuromuscular blockers. However, many SFFC medicines end up unreported and this urges the need for non-destructive techniques that could authenticate medicines instantly and flag defects in them in a cost-effective way.

Near-infrared (NIR) spectroscopy is unique in comparison to other spectroscopic techniques. As with most molecular vibrations, the fundamental frequency of vibration occurs within the mid-infrared (MIR) region of the spectrum; however, with NIR spectroscopy the overtones occur within the NIR region. The NIR region has a characteristic feature within NIR spectroscopy, which are the weak and very weak bands originating from electronic transitions and arising from vibrational overtones and combinatory modes. These overtones and combinatory modes are ‘forbidden transitions’ in terms of harmonic oscillator approximation. The weak or very weak bands are also what make this technique and region different from others and it can be an advantage when analysing samples, as there is no need for sample dilution or preparation. NIR spectra are often very complex with many overlapping peaks in diffused reflectance. However, the diffused reflectance spectrum is complex which indicates that the second derivative spectrum is appropriate for band identification purposes [15].

Near infrared-chemical imaging (NIR-CI) is a combination of NIR and image analysis used to visualise the spatial distribution of chemical compounds within a sample [16].

Table 1. WHO Alerts for SFFC Medicines (January 2022 - January 2023)

Drug Reported	Pharmaceutical Class	Country Reported	Problem	Effect of Drug
Ambroxol syrup & DOK-1 Max syrup [7]	Cough syrup	India	Substandard – Contaminated with diethylene glycol and/or ethylene glycol	Toxic and possibly lethal
Methotrex 50mg [8]	Immunosuppressant	Yemen and Lebanon	Substandard – Contaminated with pseudomonas aeruginosa	Lethal
Termorex syrup, Flurin DMP syrup, Unibebi Cough Syrup, Unibebi Demam Paracetamol Drops, Unibebi Demam Paracetamol Syrup, Paracetamol Drops, Paracetamol Syrup (mint) and Vipcol Syrup [9]	Medicinal syrups	Indonesia	Substandard – Contaminated with diethylene glycol and/or ethylene glycol	Toxic and possibly lethal
Promethazine Oral Solution, Kofexmalin Baby Cough Syrup, Makoff Baby Cough Syrup and Magrip N Cold Syrup [10]	Cough syrup	The Gambia	Substandard – Contaminated with diethylene glycol and/or ethylene glycol	Toxic and possibly lethal
Diprivan (Propofol) [11]	General anaesthetic	Venezuela	Falsified	Not reported
Dysport [12]	Neuromuscular blockers	Jordan, Turkey, Kuwait. United Kingdom, Poland	Falsified	Not reported
Intratect (Human normal immunoglobulin) [13]	Replacement therapy, immunomodulation	Brazil, India, Bolivia, Egypt	Falsified	Not reported
Desrem (Remdesivir) [14]	Antiviral	Guatemala, India	Falsified	Delay in receiving safe and effective treatment

NIR-CI offers the advantage of characterising the presence and distribution of constituents. It is an in-depth and informative technique for several applications in the pharmaceutical industry, such as process monitoring [17, 18], drug design [19–21], drug delivery [22], and counterfeit identification [23–31]. NIR-CI combines both NIR spectroscopy (NIRS) and digital imaging to produce a large amount of data from each sample [32]. The advantage of NIR-CI over NIRS is that it offers both the spatial and spectral information of each chemical component present in the sample [2]. Therefore, it can be used to detect sample homogeneity. Furthermore, it can detect low concentrations of minor components present in the sample. Also, it allows the quantitative measurement of each component without building up calibration models for the entire sample. This information is acquired at the pixel level; thus, it gives more details regarding the distribution of chemical constituents and physical properties within the sample [2, 23, 33]. Each individual pixel explains the particular data about each component; however, it is still affected by several factors [33], such as spectral radiation, instrument pixel size, and the material measured (type/sample surface/size).

Particularly for medicines, NIR-CI is used to investigate the physical properties (particle size) and chemical information regarding the presence/distribution of individual constituents, as well as the presence of contaminants within the sample [32, 33]. Due to the huge amount of data emanating from a single image, several pre-processing and multivariate data analysis methods are needed before data extraction. These include classical least square (CLS) regression, principal component analysis (PCA) [23, 24, 30], K-mean clustering [29], partial least square regression (PLSR) [24, 34], and multivariate curve resolution-alternating least square (MCR-ALS) [35–37].

Recently, the application of correlation maps to NIR-CI has been proved as a simple and powerful technique to authenticate ibuprofen branded and generic tablets, with no prior knowledge of the sample [38]. However, most of this imaging was applied after the removal of the tablets from blister packaging or destructively. Literature identifies only two studies which investigated imaging through the blister packaging of tablets to determine their water content [39] and acetyl salicylic acid [40]. Thus, the imaging of tablets through blister packaging would be advantageous as it preserves

them and allows them to be measured several times using different techniques.

The current study aims to authenticate ciprofloxacin tablets through their transparent blister packaging using NIR-CI and correlation maps. It has the following specific objectives:

1. assess the spectral features present in ciprofloxacin tablets corresponding to APIs and excipients using the correlation method,
2. identify the images of tablets through their blister packaging,
3. compare the images of whole tablets, sectioned tablets and crushed tablets
4. authenticate tested ciprofloxacin batches.

2. METHOD

Standard reference materials for APIs in ciprofloxacin tablets and the main excipients were purchased from Sigma-Aldrich. These included ciprofloxacin hydrochlorides (CIPRO) and maize starch (MAI), respectively. Additionally, three groups of ciprofloxacin tablets were measured, namely the reference authentic group (RG), test group 1 (TG1), and test group 2 (TG2). Tablets and powders were measured using a Fourier Transform (FT) NIR-CI system over the wavenumber range of 4000 – 7500 cm^{-1}, with the resolution of 4 cm^{-1}. NIR images were taken from (a) tablets inside their blister packaging, (b) coated tablets, (c) sectioned tablets, and (d) crushed tablets. Furthermore, NIR spectra of tablets (RG, TG1, and TG2), CIPRO, and MAI standards were collected. Each image was divided into 40 x 40 pixels of 70µm size and corresponded to 2.8 mm x 2.8 mm.

Spectral pre-treatment and treatment were made using Matlab (version 2019b, The MathWorks, Massachusetts) and included standard normal variate-second derivative (SNV-D2) and correlation method (CM), respectively. SNV corrected the interferences in spectra encountered due to light scattering and particle size of the sample measured [41, 42]. SNV autoclaved the absorbance values of the NIR spectrum (y) at each wavenumber (i) per the equation,

$$z_i = \frac{(y_i - \bar{y})}{s} \quad (1)$$

Where,

zi is the corrected absorbance value at the wavelength i

yi is the absorbance value at the wavelength i

$\bar{y}$ is the mean absorbance value over the full wavenumber range

s is the standard deviation of the values over the full wavenumber range

Furthermore, D2 corrected for the spectral offset and baseline encountered in the NIR spectra [41]. In this work, Savitzky-Golay D2 method was used where a polynomial of an assigned order (second degree) was fitted to the data by least squares using a number of data points (11 data points) before and after the points where a derivative is required. The process was made over the whole spectrum moving one data point each time.

For CM, correlation maps of the pixels were constructed and based on Pearson's equation [4, 38]. It was used to calculate the correlation coefficient (r) value between two spectra A and B, based on the momentum product between them (Equation 2).

$$r_p = \frac{\sum(A_i-\bar{A})\sum(B_i-\bar{B})}{\sqrt{\sum(A_i-\bar{A})^2\sum(B_i-\bar{B})^2}} \quad (2)$$

Where,

A_i is the absorbance value at each wavelength i of A

$\bar{A}$ is the mean absorbance value of A

B_i is the absorbance value at each wavelength i of B

$\bar{B}$ is the mean absorbance value of B

In this respect, the r value of the spectrum of each pixel (of each tablet) was compared to the spectra of both CIPRO and MAI. An r value = 1 indicated that both spectra were identical; whereas, a negative r value implied dissimilarity. Then, the individual r values of the pixels were used to reconstruct the maps, such that a colour code corresponded to each r value on the map. These values were then used to construct the correlation histogram for each image.

3. RESULT

Ciprofloxacin tablets used in this study had a label claim that indicated an API of ciprofloxacin hydrochloride alongside eight excipients. These

excipients in the tablet core included colloidal anhydrous silica, crospovidone, hypromellose, macrogol 400, magnesium stearate, maize starch (main excipient), microcrystalline cellulose, and titanium dioxide.

3.1. Spectral Features of Ciprofloxacin Hydrochloride, Maize Starch, and Ciproxin Tablets

The spectral features were compared for the raw spectra of CIPRO, maize starch, RG in its blister, coated RG tablet, coated TG1 tablet, and coated TG2 tablet (Figure 1). CIPRO showed key absorbance bands in two regions. The first region was between 6000 – 5500 cm^{-1} and corresponded to CH_3, CH_2, CH, ROH, and RNHR' first overtone. The second region was between 4500 – 4000 cm^{-1} and corresponded to CH_3, CH_2, and CH combination bands, respectively [41]. Figure 1a shows multiple bands corresponding to CIPRO that are not too broad, compared to MAI bands (Figure 1b). On the contrary, MAI showed broader bands with strong absorption over the full wavenumber range. MAI showed absorption bands over five main regions including 7000 – 6500 cm^{-1} (CH_3, CH_2, CH and ROH second overtone), 6000 – 5500 cm^{-1} (CH_3 first overtone), 5500 – 5000 cm^{-1} (ROH and H_2O first overtone), 5000 – 4500 cm^{-1} (ROH combination bands), and 4500 – 4000 cm^{-1} (CH_3, CH_2, CH and CHO combi-nation bands) [42]. The presence of characteristic differences in absorption bands, in turn, helped in tracking the presence or absence of CIPRO or MAI in measured tablets. Hence, RG1 tablets showed key bands corresponding both to CIPRO and MAI, whether measured through their blister packaging (Figure 1c) or directly (Figure 1d). TG1 showed corresponding bands to CIPRO and MAI, yet these bands were of poor resolution (Figure 1e), unlike TG2 that showed well-resolved bands for CIPRO and MAI.

Subsequently, the spectral quality of CIPRO, MAI, RG, TG1, and TG2 were examined. Figure 1 shows smooth spectra for most samples except CIPRO spectrum that shows noise between 5500 and 5000 cm^{-1}. The spectral offset was observed at zero for all spectra except MAI which had a slightly higher offset. Moreover, spectral background was higher in RG, TG1, and TG2 than CIPRO and MAI. The highest background was observed for RG in blister packaging, which showed that blister packaging slightly interfered in the NIR spectrum. However, this was not significant as all the peaks were prominent for RG in blister packaging. Furthermore, the tablets showed higher absorbance intensities than pure substances which ranged up to 1 absorbance units (RG and TG1). On the other hand, the

maximum number of absorbance units observed for CIPRO and MAI were 0.2 and 0.3 absorbance units, respectively.

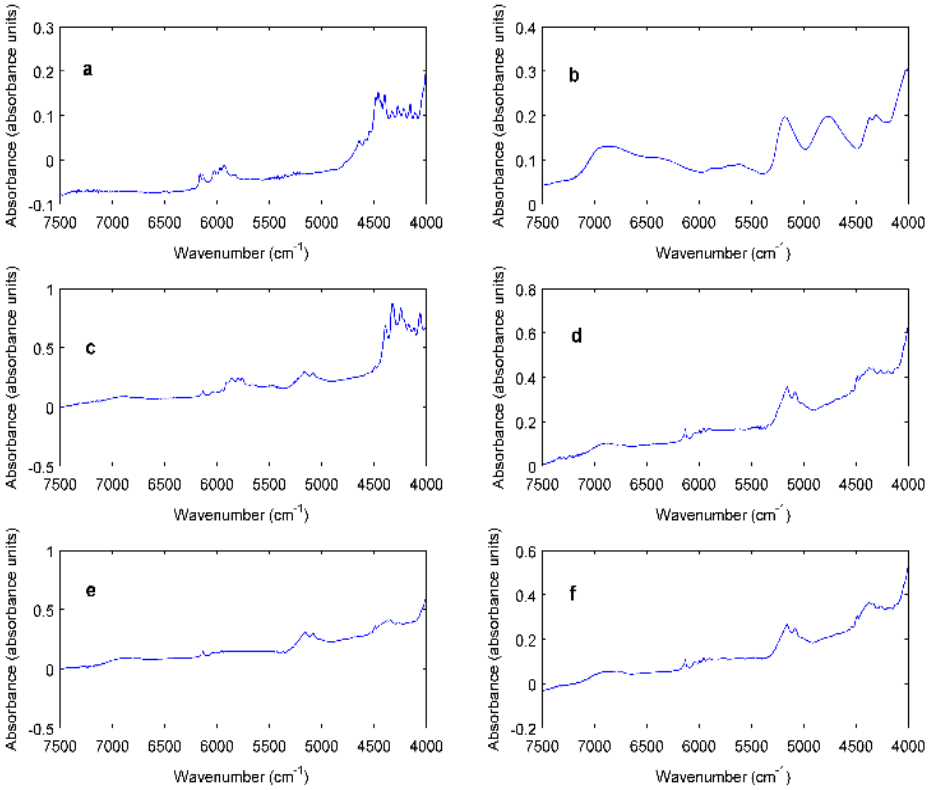

Figure 1. NIR Absorbance Spectra of (a) CIPRO, (b) MAI, (c) RG Tablet in its Blister Packaging, (d) RG Tablet not in Blister Packaging, (e) TG1, and (f) TG2 Acquired using FTNIR-CI System

The spectral features were consistent with the CM results which showed *r* values in the range of 0.77 – 0.86 for the tablets and the tablets in blister packaging against maize starch. The r values of the tablets were slightly higher against CIPRO and were above 0.9 in all the three cases. This was due to the fact that the tablets' spectra had more features for CIPRO than MAI. This fact became evident when the spectra were correlated against each other and all were found to have r values above 0.99. The value was slightly lower for the tablet in blister packaging (which was 0.92). However, the r values obtained in these cases were for the mean spectrum of each of the pure substances and tablets and did not show the individual pixels.

Consequently, the individual images of the tablet in blisters and other tablets were compared against CIPRO and MAI.

3.2. Optimising NIR Image Collection of Ciprofloxacin Tablets

Figure 2 shows the NIR image of RG tablet measured directly as well as the NIR image of RG tablet measured in its blister packaging. The image and spectral features of RG tablet were more enhanced than the tablet in blister packaging. This could be attributed to the interference in absorbance resulting from the blister packing (Figure 2). It was overcome by taking the SNV-D2 of the spectra and comparing the images of the tablets against CIPRO and MAI.

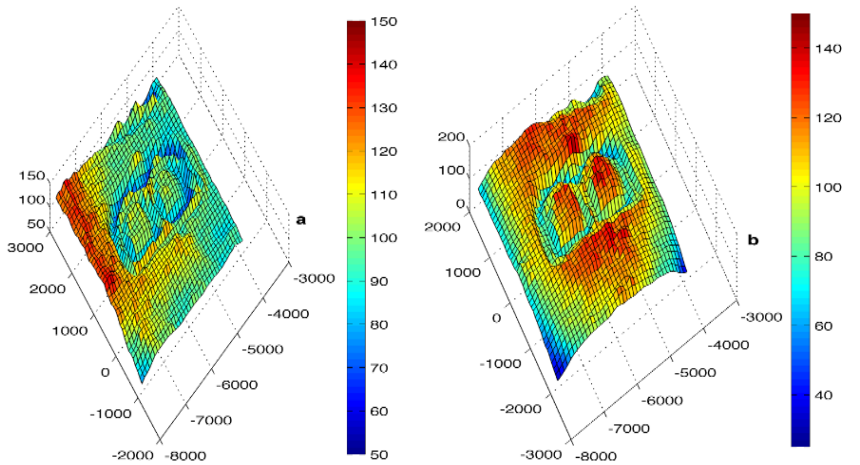

Figure 2. NIR Images of RG tablet (a) in its Blister Packaging and (b) Alone Acquired using the FT-NIR-CI System

The *r* values against CIPRO were similar for intact RG1, intact RG1 inside its blister packaging, sectioned RG1 tablet, and crushed RG1 tablet. Thus, all the four modes of the tablet showed r values in the range of 0.80 – 0.91 against CIPRO. However, r value of the RG1 tablet in its blister packaging against MAI was slightly lower than the other modes of tablet measurement. It was in the range of 0.7 – 0.75. The other modes had r values in the range of 0.8 – 0.85 against MAI. Taking the SNV-D2 spectra into account, no major difference was found in imaging the tablets through their blister packaging. Consequently, the images of the three groups of tablets

(RG, TG1 and TG2) were taken through their blister packaging prior to analysis.

3.3. Authentication of Ciprofloxacin Tablets

For the authentication of test group tablets (TG1 and TG2), correlation maps of RG, TG1, and TG2 were investigated. The correlation map of TG1 and TG2 images showed specific features related to the authenticity of tablets that conventional NIR spectroscopy did not explain. This was displayed by comparing RG, TG1, and TG2 against CIPRO and MAI. Figure 3 shows the correlation maps of each tablet image against CIPRO and MAI.

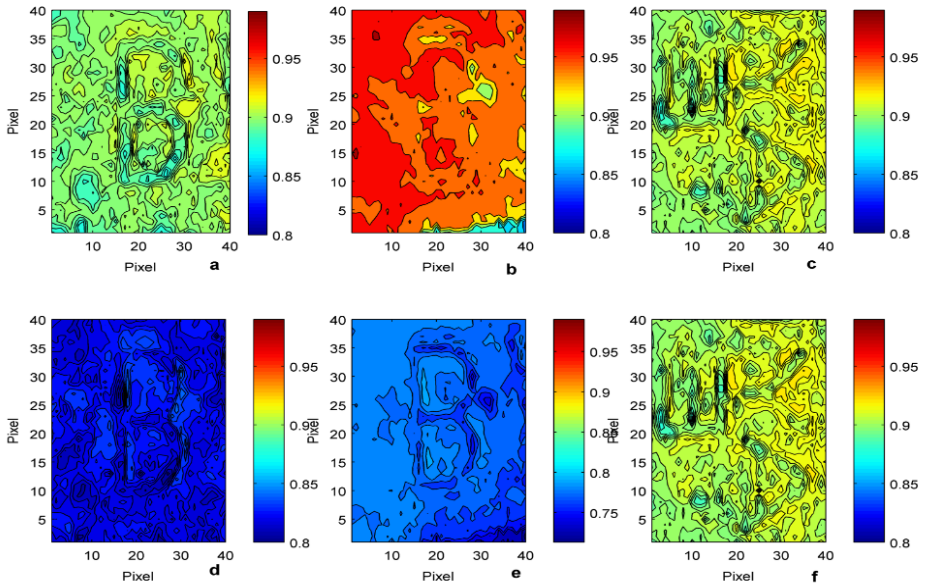

Figure 3. Correlation Maps of the Images Taken of (a) RG1 Tablet Against CIPRO, (b) TG1 Tablet (Counterfeit) Against CIPRO, (c) TG2 Tablet (Authentic) Against CIPRO, (d) RG1 Tablet Against MAI, (e) TG1 (Counterfeit) Against MAI, and (f) TG2 (Authentic) Against MAI. The r Value Range Showed a Min of 0.7 (dark blue colour) and a Max of 0.99 (Dark Red Colour)

Correlation maps showed a uniform distribution of the APIs in RG1 and TG2 but not TG1, indicating the poor content uniformity of TG1. Hence, blending procedure remained insufficient in case of TG1 and could only be

predicted using NIR-CI that allowed the detailed inspection of the whole tablet. This is due to the fact that conventional NIRS gives an overview of the whole measured sample; whereas, NIR-CI informs about the spatial distribution of the components within the sample [43]. In this respect, correlation maps showed dark red colour for r values in the range of 0.95 – 0.99 (maximum); whereas, dark blue colour corresponded to r values in the range of 0.75 – 0.85 (minimum). Against CIPRO, the three groups of tablets (RG, TG1 and TG2) showed r values in the range of 0.85 – 0.99. However, RG and TG2 showed higher similarity in the distribution of r values on the maps and had r values in the range of 0.85 – 0.93 (Figures 1a and 1c). On the other hand, r values were slightly elevated for TG1 map and were in the range of 0.85 – 0.98. Similarly, the r values of TG1 against MAI were lower than the other two tablets and were in the range of 0.7 – 0.8. However, RG and TG2 showed r values against MAI between 0.8 and 0.95. Subsequently, TG1 tablets failed the manufacturer's specification in terms of having a higher amount and inconsistent distribution of APIs, as well as a lower amount of the main excipient. In this case, NIR-CI was combined with correlation maps that indicated the differences in the distribution and intensities of each pixel in each tablet against CIPRO and MAI.

3.4. Histogram Analysis of Correlation Maps

A histogram was constructed representing the number of pixels corresponding to each r value between 0.5 – 0.8 for each image (Figure 4). Histograms showed high similarity between the pixels of RG and TG2. Thus, 784 pixels of RG had r = 0.90 against CIPRO. Additionally, the remaining pixels had r values of 0.91, 0.89, and 0.85 which corresponded to 91, 610, and 114 pixels, respectively (Figure 4a). This distribution was similar for TG2 which showed r values of 0.92, 0.91, 0.90, 0.89, and 0.85, corresponding to 46, 528, 755, 237, and 32 pixels, respectively (Figure 4c). However, TG2 showed a different distribution of pixels related to 11 r values between 0.85 and 0.98 (Figure 4b). Most of the pixels (n = 923) had r values of 0.95 and 0.96, which was notably different from the histograms of RG and TG2 tablets. This further confirmed that TG1 could be a substandard or counterfeit medicine, although it still needs confirmation by further analysis.

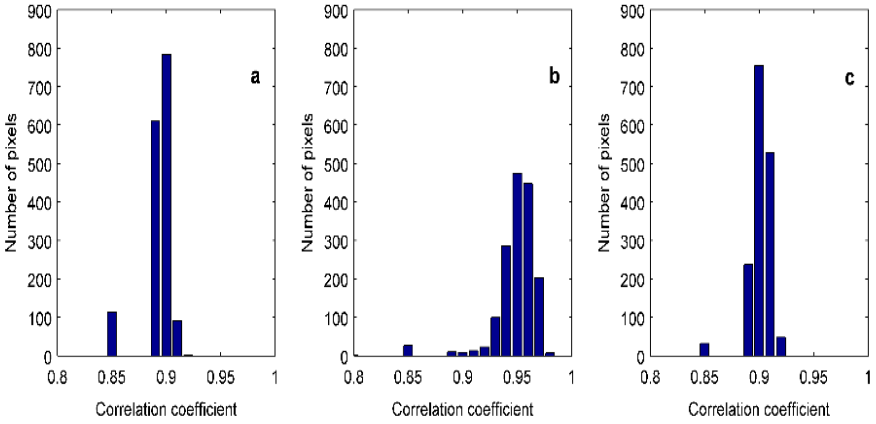

Figure 4. Histogram of the Correlation Coefficient Values Against the Number of Pixels of (a) RG1 Tablet, (b) TG1 Tablet, (c) TG2 Tablet Against CIPRO.

4. DISCUSSION

Fluoroquinolones belong to a class of antibiotics used to treat or prevent certain bacterial infections. The most common type of fluoroquinolone used is ciprofloxacin. It is a highly counterfeited medicine which is often prescribed due to its efficiency, safety, and relatively low cost [44]. According to the University of Oxford, the global antibiotic consumption increased by 46% between 2000 and 2018 across 204 countries [45]. This demand for antibiotics has led to an increased number of counterfeit ciprofloxacin being sold globally and often being purchased by unsuspecting customers [46–48]. South Asia had some of the highest consumption rates for fluoroquinolone during the eighteen-year period observed by the University of Oxford, with numbers increasing 1.8-folds [45]. The oversubscribing of ciprofloxacin (amongst other antibiotics) and the availability of sub-standard or falsified medicines in developing countries has contributed towards the increased risk of antibiotic resistance, worldwide [49, 50]. According to the WHO [51], the rate of resistance to ciprofloxacin varied from 8.4% to 92.9% for Escherichia coli and from 4.1% to 79.4% for Klebsiella pneumoniae in countries reporting to the Global Antimicrobial Resistance and Use Surveillance System (GLASS). Researchers have identified that 1.27 million deaths worldwide could be attributed to antimicrobial resistance, out of 4.95 million recorded cases [52]. Although, not all these deaths are because of counterfeit and

substandard medicines, still many of them could be. Hence, further study into the use of NIR and counterfeit medicines could prove extremely beneficial in combatting the issue, globally.

The findings of the current study demonstrated the power of NIR-CI to provide a comprehensive authentication approach for medicines based on their chemical and physical differences. This is important, particularly in the case of antibiotics, where it is necessary to deliver the correct dose to the patients to optimise therapeutic outcomes [53].

In the current work, ciprofloxacin was used as a model considering its widespread use. Ciprofloxacin tablets contain multiple excipients (n = 8) in addition to APIs. Ciprofloxacin belongs to the class of fluoroquinolones and is commonly used to treat gram-negative infections, such as pneumonia [54]. Ciprofloxacin tablets used in this study contained more than 50% m/m of ciprofloxacin hydrochloride and were oval-shaped, film-coated, white tablets with a score line in the middle. The presence of the score line in the middle allows for two options in the intake of tablets. These options include (1) taking the tablet as a whole if a full-dose is required and (2) splitting the tablet in half if half a dose is required. In cases where half a dose is required, ensuring content uniformity and homogenous distribution of APIs and excipients in the tablet is important.

Subsequently, NIR-CI was used as an analytical technique to assess non-destructively the homogeneity of the content of authentic (RG) and test ciprofloxacin (TG1 and TG2) tablets. NIR-CI yielded 3D-datasets that encompassed spectral hypercubes of x, y, and z dimensions. In this respect, x and y axis showed spatial data, while z axis indicated spectral data [32]. The 3D-datasets indicated the homogeneity of each of the three groups (RG, TG1, and TG2), which could not be established using conventional NIRS. Conventional NIRS, especially in diffused reflectance mode, can assess the presence/amount of APIs and excipients but not their individual distribution [41].

Furthermore, NIR-CI offers a further advantage over NIRS in the detection of analytes due to the array-based spectral sensing of the NIR-CI systems, where spectral parallel data collection is not affected by the dilution effect of bulk measurement [32]. This is why in previous studies NIR-CI acted as an ideal technique for inspecting spatial distribution of constituents in the tablets [29, 43, 55], monitoring blending uniformity [56],

and monitoring manufacturing processes [57–59]. Likewise, in this study, NIR-CI was successful and sensitive in examining the content uniformity of CIPRO and MAI in ciprofloxacin tablets, when measured inside their blister packaging. Blister packaging did interfere with the offset and background of raw tablets spectra. Nonetheless, this interference was successfully removed using SNV-D2 pretreatment algorithm applied in NIR spectral correction in other studies [60].

By comparing the SNV-D2 spectra using CM algorithm, NIR-CI accurately indicated the distribution of CIPRO and MAI in tablets via the correlation maps (images). In this respect, CM showed the degree of similarity of the individual components of the tablets' NIR spectra to CIPRO and MAI, accurately [42]. This was further confirmed by plotting the histogram of the r values of tablets against CIPRO. TG1 tablet showed an over-dose of CIPRO that was not uniformly distributed, while TG2 showed a similar distribution to RG indicating the correct dose of CIPRO. This, in turn, pointed out that TG1 could be a counterfeit/substandard medicine containing a higher dose of APIs than claimed by the label.

4.1. Conclusion

This study evaluated NIR-CI to authenticate the test ciprofloxacin tablets. Authentic tablets showed an exact match of CIPRO and the main excipient against the reference tablets. Counterfeit/substandard tablets showed key differences in the amount of CIPRO and their distribution against the reference tablets. Information corresponding to CIPRO was featured in the ranges 6200 – 5500 and 4500 – 4000 cm-1, respectively. It was traced in all tablets. However, the histogram of counterfeit/substandard tablets showed a shift to the right with an increase in r values, when compared to reference and authentic tablets. This established that tablet quality could be traced using the skewness of the histogram. The skewness of the image showed further usefulness in spotting a counterfeit/substandard medicine.

4.2. Limitations

The current study has some limitations. The first limitation was related to sample size based on which only three groups of tablets (one reference and two test tablets) were investigated. Moreover, the imaging system used was slow, although it was non-destructive and able to identify tablets inside blister packaging. Due to its slow speed, the collection of each image

required 8-10 hours. Future research work may apply NIR-CI to a larger sample size and different classes of antibiotics.

REFERENCES

1. World Health Organization. 1 in 10 medical products in developing countries is substandard or falsified. WHO Web site. https://www.who.int/news/item/28-11-2017-1-in-10-medical-products-in-developing-countries-is-substandard-or-falsified. Updated November 28, 2017. Accessed December 26, 2022.
2. Moffat AC, Assi S, Watt RA. Identifying counterfeit medicines using near-infrared spectroscopy. *J Near Infrared Spectrosc*. 2010;18(1):1–15.
3. World Health Organisation. Substandard and falsified medical products. WHO Web site. https://www.who.int/news-room/fact-sheets/detail/substandard-and-falsified-medical-products. Updated January 31, 2018. Accessed December 26, 2022.
4. Assi S, Watt RA, Moffat AC. Identification of counterfeit medicines from the internet and the world market using near-infrared spectroscopy. *Anal Methods*. 2010; 3:2231–2236. https://doi.org/10.1039/C1AY05227F
5. Wertheimer AI, Santella TM. Drug counterfeiting: The current situation and prevention strategies for the future. *Int J Pharm Med*. 2005;19:301–308. https://doi.org/10.2165/00124363-200519050-00007
6. World Health Organisation. Full list of WHO medical product alerts. WHO Web site. https://www.who.int/teams/regulation-prequalification/incidents-and-SF/full-list-of-who-medical-product-alerts. Updated January 11, 2023. Accessed January 25, 2023.
7. World Health Organisation. Medical product alert N°1/2023: Substandard (con-taminated) liquid dosage medicines. WHO Web site. https://www.who.int/news/item/11-01-2023-medical-product-alert-n-1-2023-substandard-(contaminated)-liquid-dosage-medicines. Updated January 11, 2023. Accessed January 25, 2023.
8. World Health Organisation. Medical product alert N°8/2022: Substandard (contaminated) METHOTREX 50mg. WHO Web site. https://www.who.int/news/item/27-12-2022-medical-product-alert-n-

8-2022-substandard-(contaminated)-methotrex. Updated December 27, 2022. Accessed January 25, 2023.

9. World Health Organisation. Medical product alert N°7/2022: Substandard (contaminated) paediatric liquid dosage medicines. WHO Web site. https://www.who.int/news/item/02-11-2022-medical-product-alert-n-7-2022-substandard-(contaminated)-paediatric-liquid-dosage-medicines. Updated November 2, 2022. Accessed January 25, 2023.
10. World Health Organisation. Medical product alert N°6/2022: Substandard (contaminated) paediatric medicines. WHO web site. https://www.who.int/news/item/05-10-2022-medical-product-alert-n-6-2022-substandard-(contaminated)-paediatric-medicines. Updated October 5, 2022. Accessed January 25, 2023.
11. World Health Organisation. Medical product alert N°5/2022: DIPRIVAN. WHO Web site. https://www.who.int/news/item/25-08-2022-medical-product-alert-n-5-2022-falsified-diprivan. Updated August 25, 2022. Accessed January 25, 2023.
12. World Health Organisation. Medical product alert N°4/2022: Falsified DYSPORT. WHO Web site. https://www.who.int/news/item/19-08-2022-medical-product-alert-n-4-2022-falsified-dysport. Updated August 19, 2022. Accessed January 25, 2023.
13. World Health Organisation. Medical product alert N°3/2022: Falsified intratect (Human normal immunoglobulin). WHO Web site. https://www.who.int/news/item/27-05-2022-medical-product-alert-n-3-2022-falsified-intratect-human-normal-immunoglobulin. Updated May 27, 2022. Accessed January 25, 2023.
14. World Health Organisation. Medical product alert N°2/2022: Falsified DESREM (Remdesivir). WHO Web site. https://www.who.int/news/item/09-03-2022-medical-product-alert-n-2-2022-falsified-desrem-(remdesivir). Updated March 9, 2022. Accessed January 25, 2023.
15. Y Ozaki, K Awa, D Ishikawa. Near-infrared spectroscopy in biological molecules and tissues. In: Moffat AC, Osselton MD, Elliott SP, eds. *Clarke's Analysis of Drugs and Poisons*. London: Pharmaceutical Press; 2018.

16. Ravn C, Skibsted E, Bro R. Near-infrared chemical imaging (NIR-CI) on pharmaceutical solid dosage forms-comparing common calibration approaches. *J Pharm Biomed Anal*. 2008;48(3):554–561. https://doi.org/10.1016/j.jpba.2008.07.019

17. Li W, Woldu A, Kelly R, et al. Measurement of drug agglomerates in powder blending simulation samples by near infra-red chemical imaging. *Int J Pharm*. 2008;350(1-2):369–373. https://doi.org/10.1016/j.ijpharm.2007.08.055

18. Hilden L, Pommier CJ, Badawy S, Friedman EM. NIR chemical imaging to guide/ sup-port BMS-561389 tablet formulation development. *Int J Pharm*. 2008;353:283–290. https://doi.org/10.1016/j.ijpharm.2007.11.032

19. Shah RB, Tawakkul MA, Khan MA. Process analytical technology: Chemometric analysis of Raman and near infra-red spectroscopic data for predicting physical properties of ex-tended release matrix tablets. *J Pharm Sci*. 2007;96(5):1356–1365. https://doi.org/10.1002/jps.20931

20. Ellison CD, Ennis BJ, Hamad ML, Lyon RC. Measuring the distribution of density and tabletting force in pharmaceutical tablets by chemical imaging. *J Pharm Biomed Anal*. 2008;48(1):1–7. https://doi.org/10.1016/j.jpba.2008.04.020

21. Hammond SV, Clarke FC. *Handbook of Vibrational Spectroscopy*. London: John Wiley & Sons; 2002.

22. Clarke F. Extracting process-related information from pharmaceutical dosage forms using near infrared microscopy. *Vib Spectrosc*. 2004;34:25–35. https://doi.org/10.1016/j.vibspec.2003.08.005

23. Gendrin C, Roggo Y, Collet C. Pharmaceutical applications of vibrational chemical imaging and chemometrics: A review. *J Pharm Biomed Anal*. 2008;48(3):533–553. https://doi.org/10.1016/j.jpba.2008.08.014

24. Dubois J, Wolff JC, Warrack JK, Schoppelrei J, Lewis EN. NIR chemical imaging for counterfeit pharmaceutical products analysis. *Spectrosc*. 2007;22:40–50.

25. Westenberger BJ, Ellison CD, Fussner AS, et al. Quality assessment of internet pharmaceutical products using traditional and non-traditional

analytical techniques. *Int J Pharm*. 2005;306(1-2):56–70. https://doi.org/10.1016/j.ijpharm.2005.08.027

26. Veronin MA, Lee E, Lewis EN. "Insight" into drug quality: Comparison of simvastatin tablets from the US and Canada obtained via the internet. *Ann Pharmacother*. 2007;41(7-8):1111–1115. https://doi.org/10.1345/aph.1H680
27. Veronin MA, Youan BBC. Magic bullet gone astray: Medications and the internet. *Science*. 2004;305(5683):481. https://doi.org/10.1126/science.1097355
28. Wolf JC, Warrack JK. NIR-based chemical imaging as an anticounterfeiting tool. *Pharma Manufacturing*. 2007:1–5.
29. Lopes MB, Wolff JC. Investigation into classification/ sourcing of suspect counterfeit Hep-todin tablets by near infrared chemical imaging. *Anal Chim Acta*. 2009; 633(1):149–155. https://doi.org/10.1016/j.aca.2008.11.036
30. Lopez MB, Wolf JC, Bioucas-Dias JM, Figueiredo MAT. Determination of the composition of counterfeit Heptodin tablets by near infrared chemical imaging and classical least square estimation. *Anal Chim Acta*. 2009;641(1-2):46–51. https://doi.org/10.1016/j.aca.2009.03.034
31. Sabin GP, Lozano VA, Rocha WFC, Romao W, Ortiz RS, Poppi RJ. Characterisation of sildenafil citrate tablets of different sources by near infrared chemical imaging and chemo-metric tools. *J Pharm Biomed Anal*. 2013;85:207–212. https://doi.org/10.1016/j.jpba.2013.07.036
32. Reich G. Near-infrared spectroscopy and imaging: Basic principles and pharmaceutical ap-plications. *Adv Drug Delivery Rev*. 2005;57(8):1109–1143. https://doi.org/10.1016/j.addr.2005.01.020
33. Amigo JM. Practical issues of hyperspectral imaging analysis of solid dosage forms. *Anal and Bioanal Chem*. 2010;398:93–109. https://doi.org/10.1007/s00216-010-3828-z
34. Puchert T, Lochmann D, Menezes JC, Reich G. Near-infrared chemical imaging (NIR-CI) for counterfeit drug identification—A four-stage concept with a novel approach of data pro-cessing (Linear Image

Signature). *J Pharm Biomed Anal*. 2010;51(1):138–145. https://doi.org/10.1016/j.jpba.2009.08.022

35. Amigo JM, Cruz J, Bautista M, Maspoch S, Coello J, Blanco M. Study of pharmaceutical samples by NIR chemical-image and multivariate analysis. *Trac-Trend Anal Chem*. 2008;27(8):696–713. https://doi.org/10.1016/j.trac.2008.05.010
36. Amigo JM, Ravn C. Direct quantification and distribution assessment of major and minor components in pharmaceutical tablets by NIR-chemical imaging. *J Pharm Sci*. 2009;37(2):76–82. https://doi.org/10.1016/j.ejps.2009.01.001
37. Ravn C, Bro E. Near-infrared chemical imaging (NIR-CI) on pharmaceutical solid dosage forms—Comparing common calibration approaches. *J Pharm Biomed Anal*. 2010;48(3):554–561. https://doi.org/10.1016/j.jpba.2008.07.019
38. Cairos C, Amigo JM, Watt R, Coello J, Maspoch S. Implementation of enhanced correla-tion maps in near infrared chemical images: Application in pharmaceutical research. *Talanta.* 2009;79(3):657–664. https://doi.org/10.1016/j.talanta.2009.04.042
39. Malik I, Poonacha M, Moses J, Lodder RA. Multispectral imaging of tablets in blister packaging. *AAPS PharmSciTech*. 2001;2(2):1–7.
40. Hamilton SJ, Lowell AE, Lodder RA. Hyperspectral imaging technology for pharmaceutical analysis. *J Biomedical Opt*. 2002;7:561–570. https://doi.org/10.1117/12.472076
41. Jee RD. Near-infrared spectroscopy. In: Moffat AC, Osselton MD, Elliot SP, eds. *Clarke's Analysis of Drugs and Poisons in Pharmaceutical Body Fluids Postmortem Material*. Pharmaceutical Press; 2011.
42. Varmuza K, Filzmoser P. *Introduction to Multivariate Statistical Analysis in Chemometrics*. Boca Raton: Taylor & Francis Group; 2009.
43. Koehler FW, Lee E, Kidder LH, Lewis EN. Near infrared spectroscopy: The practical chemical imaging solution. *Spectrosc Eur*. 2002;14(3): 12–19.

44. Byarugaba DK. Antimicrobial resistance in developing countries and responsible risk factors. *Int J Antimicrob Agents*. 2004;24(2):105–110. https://doi.org/10.1016/j.ijantimicag.2004.02.015

45. Conley ZC, Bodine TJ, Chou A, Zechiedrich L. Wicked: The untold story of ciprofloxacin. *PLoS Pathog*. 2018;14(3):e1006805. https://doi.org/10.1371/journal.ppat.1006805

46. University of Oxford. Global antibiotic consumption rates increased by 46 percent since 2000. University of Oxford Web site. https://www.ox.ac.uk/news/2021-11-16-global-antibiotic-consumption-rates-increased-46-percent-2000. Updated November 16, 2021. Accessed January 26, 2023

47. Bhatti MW. Alarming threat: Probe launched after counterfeit medicines found in Hyderabad, Lahore. *The News International*. September 12, 2022. https://www.thenews.com.pk/print/990593-alarming-threat-probe-launched-after-counterfeit-medicines-found-in-hyderabad-lahore. Accessed January 26, 2023.

48. Taylor NP. Asia-Pacific roundup: Malaysia's MDA posts draft guidance on custom-made medical devices. *Regulatory Focus*. November 1, 2022. https://www.raps.org/news-and-articles/news-articles/2022/11/asia-pacific-roundup-malaysias-mda-posts-draft-gui. Accessed January 26, 2023.

49. NAFDAC blacklists Indian company over fake ciprofloxacin. *Premium Times*. October 27, 2020. https://www.premiumtimesng.com/news/more-news/423277-nafdac-blacklists-indian-company-over-fake-ciprofloxacin.html. Accessed January 26, 2023.

50. Zabala GA, Bellingham K, Vidhamaly V, et al. Substandard and falsified antibiotics: Neglected drivers of antimicrobial resistance? *BMJ Global Health*. 2022;7(8):e008587. http://dx.doi.org/10.1136/bmjgh-2022-008587

51. Sharma D, Patel RP, Zaidi STR, Sarker MMR, Lean QY, Ming LC. Interplay of the quality of ciprofloxacin and antibiotic resistance in developing countries. *Front Pharmacol*. 2017;8:546. https://doi.org/10.3389/fphar.2017.00546

52. World Health Organisation. Antimicrobial resistance. WHO Web site. https://www.who.int/news-room/fact-sheets/detail/antimicrobial-resistance. Updated November 17, 2021. Accessed January 26, 2023.

53. Shukla D. Antimicrobial resistance 'is not an abstract threat lurking in the shadows'. *Medical News Today*. January 29, 2022. https://www.medicalnewstoday.com/articles/antimicrobial-resistance-is-not-an-abstract-threat-lurking-in-the-shadows. Accessed 26 January, 2023.

54. Zhang HL, Tan M, Qiu AM, Tao Z, Wang CH. Antibiotics for treatment of acute exacerbation of chronic obstructive pulmonary disease: A network meta-analysis. *BMC Pulm Med*. 2017;17(1):e196. https://doi.org/10.1186/s12890-017-0541-0

55. Clark F. NIR microscopy: Utilization from research through to full-scale manufacturing. Presented at: The European Conference on Near-infrared Spectroscopy; 2003; Heidelberg.

56. Rodionova OY, Houmoller LP, Pomerantsev P, et al. NIR spectrometry for counterfeit drug detection a feasibility study. *Anal Chem Acta*. 2005;549(1-2):151–158. https://doi.org/10.1016/j.aca.2005.06.018

57. Wu Z, Tao O, Cheng W, Yu L, Shi X, Qiao, Y. Visualizing excipient composition and homogeneity of Compound Liquorice tablets by near-infrared chemical imaging. *Spectrochim Acta A*. 2012;86:631–636. https://doi.org/10.1016/j.saa.2011.10.030

58. Khorasani M, Amigo JM, Sun CC, Bertelsen P, Rantanen J. Near-infrared chemical imaging (NIR-CI) as a process monitoring solution for a production line of roll compaction and tableting. *Eur J Pharm Biopharm*. 2015;93:293–302. https://doi.org/10.1016/j.ejpb.2015.04.008

59. Wahl PR, Pucher I, Scheibelhofer O, Kerschhaggl M, Sacher S, Khinast JG. Continuous monitoring of API content, API distribution and crushing strength after tableting via near-infrared chemical imaging. *Int J Pharm*. 2017;518(1-2):130–137. https://doi.org/10.1016/j.ijpharm.2016.12.003

60. Boldrini B, Kessler W, Rebner K, Kessler RW. Hyperspectral imaging: A review of best practice, performance and pitfalls for in-line and on-line applications. *J Near Infrared Spectrosc*. 2012;20(5):483–508.